23

(NASA-CR-115585) RESEARCH ON LUNAR METERIALS Final Report, 3 Jun. 1968 - 31 Jan. 1971 (Cornell Univ.) Apr. 1971 41 p
CSCL C3B
G3/30

N72-24869
thru
N72-24871
Unclas
28829

CR-115585

CORNELL UNIVERSITY

Center for Radiophysics and Space Research

ITHACA, N. Y.

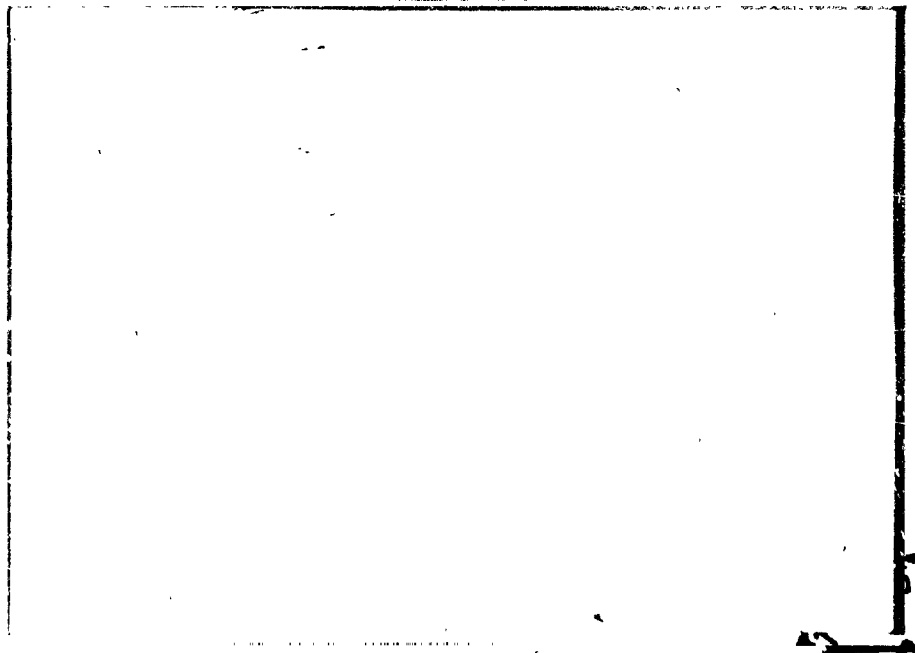

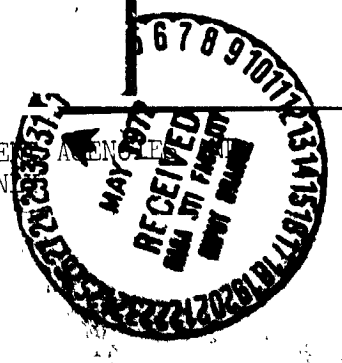

U.S. GOVERNMENT AGENCIES AND CONTRACTORS ONLY

OFFICE OF PRIME RESPONSIBILITY

TA3

CENTER FOR RADIOPHYSICS AND SPACE RESEARCH
CORNELL UNIVERSITY
ITHACA, NEW YORK

April 1971

CRSR 435

Final Report

to the

NATIONAL AERONAUTICS AND SPACE ADMINISTRATION

NASA Contract NAS9-8018

RESEARCH ON LUNAR MATERIALS

June 3, 1968 through January 31, 1971

Administrative Report--not for general distribution

1. Introduction

This report consists of two papers presented at the First and Second Annual Lunar Science Conference at Houston in January 1970 and January 1971.

1. "Optical and High Frequency Electrical Properties of the Lunar Sample." This paper describes the experimental work and observations on the Apollo 11 lunar samples. It was published in Science (167, p. 707, 1970) and in the Proceedings of the Apollo 11 Lunar Science Conference, A.A. Levinson, ed. (Pergamon Press, p. 2149, 1970).

2. "Some Physical Properties of the Apollo 12 Lunar Samples." This paper summarizes our findings on the Apollo 12 samples and compares certain experimental results obtained in the Apollo 11 and Apollo 12 samples. It is going to be published in the Proceedings of the Apollo 12 Lunar Science Conference.

SOME PHYSICAL PROPERTIES OF APOLLO 12 LUNAR SAMPLES

T. Gold, B. T. O'Leary and M. Campbell
Center for Radiophysics and Space Research
Cornell University
Ithaca, New York 14850

January 1971

N72-24870

ABSTRACT--The size distribution of the lunar fines is measured, and small but significant differences are found between the Apollo 11 and 12 samples as well as among the Apollo 12 core samples. The observed differences in grain size distribution in the core samples are related to surface transportation processes, and the importance of a sedimentation process versus meteoritic impact "gardening" of the mare grounds is discussed. The optical and the radio frequency electrical properties are measured and are also found to differ only slightly from Apollo 11 results.

APOLLO 12 GRAIN SIZE ANALYSIS

The Apollo 12 lunar fines were subjected to similar grain size analysis to that carried out for the Apollo 11 sample (Gold et al., 1970). The general appearance and the appearance under the microscope of all samples of fines are rather similar, and the measured optical properties also show only small but significant differences. Although this type of uniformity was expected as a consequence of ground-based optical observations of the moon (Hapke, 1968), it nevertheless has to be emphasized as a remarkable conclusion.

The particle size distribution has been determined by two methods: electron microscopy and sedimentation rate in a column of water. The first was described in the Apollo 11 report (Gold et al., 1970) and is of greatest value for particle sizes ranging down from 10 microns to less than 0.1 micron; it utilizes scanning electron micrographs of small "sections" of powder. The second method utilizes a sedimentation column which has been improved and perfected more recently.

The water sedimentation column consists of a vertical pipe 70.9 cm long, terminating below in a cubical box of optical glass plate. A photographic flash gun is imaged through a large aperture lens with focus just below the point of entry of the tube. Flash synchronized photographs are taken in a viewing direction perpen-

dicular to the direction of the light. Stray and multiply scattered light is carefully excluded, and as a result the light scattered by a particle as small as 1 micron gives a perfectly recordable image. The water column is heated at the top and the temperature distribution along it is carefully controlled so that no thermal convection can set in. The particle sizes are deduced by Stokes' Law assuming them to be spherical. While this is of course not accurate, the optical and electron microscope examination showed the particles to be on the whole rather compact shapes, making this error rather small. Freedom from disturbing convection in the column is demonstrated by taking the photographs in pairs with a short duration in between, showing that each group of particles has settled a distance in that short time appropriate to its settling time from the top.

For an absolute measurement this method would perhaps not be sufficiently accurate, both for reasons of the particle shapes and perhaps also their unknown densities. For a comparison the method is very good, and it is much easier to accumulate good statistics than by the method of counting particles under the microscope.

Fig. 1 compares the small-size particle size distribution of the Apollo 11 bulk box with that of the Apollo 12 contingency sample; the data, obtained by electron microscopy, are plotted as the cumulative number, per cubic centimeter, of particles larger in size than the abscissa value. A porosity of 0.5 is assumed and the number of particles counted is about 2000 in each case. The two curves are very similar, showing greatest divergence at particle

sizes of a few microns; the difference, which amounts to less than a factor 2.5, is probably real. Its significance is shown a little more clearly in Fig. 2 in which the differential rather than cumulated particle density is plotted.

The Apollo 12 contingency sample and three core samples (from cores 12025 and 12028) have been analyzed by the sedimentation column method, and the comparisons are shown on Figs. 3 and 4. From these curves it would appear that the surface sample from Apollo 12 is slightly coarser grained than that from Apollo 11. Among the core samples there is also a variation in the grain size distribution, with the deeper samples being somewhat richer in small particles than the surface and close subsurface ones. In particular the sample taken from a trench 15 cm deep (sample 12033) is significantly different in appearance from most others, and the size distribution analysis shows this one to possess a much larger proportion of small particles.

Figs. 5 and 6 compare grain size analysis data obtained by the two different methods.

The fact that the grain size distribution in the core sample shows significant differences within tens of centimeters variation of depth requires comment. Differences over intervals of some centimeters in the core sample are also seen in the albedo (note color differences reported by the Lunar Sample Preliminary Examination Team, 1970), and very striking chemical differences have been reported (E. Anders, 1971). One has to discuss how sharply defined layers or other local configurations could be preserved despite the fact that some plowing of the ground by meteoritic impact must be taking place.

A material of different grain size, albedo or chemical composition could be deriv[illegible] fr[illegible] [illegible]ffici[illegible]tly dist[illegible]nt

or deep crater for this material not to have been previously well mixed by meteorite impact, or it could be material that is different as a result of contamination with some direct meteoritic infall. But it is not enough to account for possible sources of such different material. One must also understand firstly how it can have been deposited without excessive mixing, and secondly how it can have avoided being mixed by the plowing over which meteorites must be causing on the lunar surface.

The deposition of the material must be gentle and it cannot have reached its present position by being flung there on ballistic trajectories from a distant and deep crater. A layer some centimeters thick could not be deposited from such ballistic trajectories without mixing with a layer very many times its own thickness. The material seen in the core must thus have reached its position by a surface transportation process resulting in a sufficiently gentle sedimentation to avoid mixing. Secondly, in order to preserve such layers, one has to suppose that further sedimentation has taken place so that the overburden can protect the layer from meteorite plowing. If the rate of the meteorite plowing process were known, one could conclude what the rate of deposition has to be to have a significant probability that a layer at a given depth would be seen preserved. It is quite clear that even a single example of a very inhomogeneous core demonstrates that the ground has not been turned over hundreds of times to these depths, as had been calculated from estimates of the meteoritic infall rate. The mare ground seems to be subject to a sedimentation process much more than to a "gardening" process.

DIELECTRIC CONSTANT MEASUREMENT

The measurements of the high frequency electrical properties at 450 MHz were made by the same methods employed for the Apollo 11 samples (Gold et al., 1970 ; Campbell and Ulrichs, 1969). Moisture effects were avoided by having solid samples cut dry in laboratory atmosphere; as a precaution these were vacuum baked at 120°C for two days. Powder samples were stored in a dessicator with a large excess of anhydrous silica gel. The results do not disclose any marked difference in the dielectric constant of powder material from site to site. In Fig. 7 the dielectric constant measurements, as a function of bulk powder density, are shown for two Apollo 12 sites--one at a depth of 15 cm below the surface--as well as for the Apollo 11 bulk sample. The two Apollo 12 samples were chosen for their contrasting physical appearances, sample 12033 being much lighter in color and finer in texture than sample 12070. The variation of dielectric constant with density follows the Rayleigh formula (Campbell and Ulrichs, 1969) in all cases and, indeed a single such curve fits all the data within ±1 percent excepting only the highest density point of sample 12070. The ground-based radar determinations of the dielectric constant (see Evans and Hagfors, 1968) are in complete accord with these measurements if one assumes a density of about 1.7 g cm^{-3} for the soil at a depth of 20 cm, an assumption which does no violence to the known properties of the soil.

Also shown on Fig. 7 are dielectric constant--density points for four solid lunar rocks, two each from Apollos 11 and 12. The

latter pair, 12063 and 12065, are very similar petrologically and lie closely adjacent in the figure. Some allowance should be made for the porosity (~15%) of sample 10022 but this cannot greatly change the scatter of the points corresponding to this small but not atypical selection of rocks. None of the four solid rocks, nor any mixture of them, could be ground to a powder with the electrical properties (dielectric constant and loss tangent) of the dust samples, a conclusion in which

we concur with the mineralogists.

Fig. 8 shows in a similar way the variations with density of the absorption length in the powder samples, with points for the four solid rocks in addition. Again, assuming plausible densities for the powder at depths of a few centimeters, the data agree with prior ground-based radiothermal observations by Krotikov and Troitsky (1963) and others.

OPTICAL PROPERTIES

The optical reflectivity and polarization of the Apollo 12 soil sample were measured as a function of phase angle with the same instrument and in the same manner as done previously for the Apollo 11 samples (O'Leary and Briggs, 1970). Both Apollo 11 and 12 samples were prepared by gradually dropping the fine-grained soil from a height of about 2 cm onto a sample tray.

Figs. 9 and 10 indicate the dependence of reflectivity and polarization on phase angle for two viewing angles, ϵ, of 0° and 60°, as measured from the normal to the surface of the sample. While the Apollo 11 and 12 samples have similar photometric curves, the Apollo 12 sample is noticeably brighter than Apollo 11 (Fig. 9). The curves labeled "Moon" are taken from Hapke (1968) and normalized to the normal albedo of the Apollo 11 sample. The Apollo 12 soil has a normal albedo at .56 μm wavelength of .125±.003 as compared with.102±.003 for the Apollo 11 sample. Moreover, the Apollo 12 soil is redder than both the Apollo soil and the mean value for the moon (Gehrels et al., 1964). Finally, the Apollo 12 soil shows greater reddening with phase angle than the Apollo 11

soil. At $\epsilon=60^{\circ}$, the photometric functions of both the Apollo 11 and 12 soils indicate a flattening toward larger phase angles compared with the lunar curve. The difference can probably be attributed to large scale roughness of the lunar surface as observed from the earth.

In Fig. 10 the polarization of the Apollo 12 soil is very similar to that of the moon as a whole (Hapke, 1968). However, for $\epsilon=60^{\circ}$, both samples show peaks in polarization at greater phase angles than for the moon (Pellicori, 1969). The maximum polarization from the Apollo 12 sample is in good agreemen with earth-based observations, while that of Apollo 11 is anomalously high. The interpretation of these data is somewhat uncertain, however, because of such factors as compaction, interaction with moisture and relative quantities of surface and subsurface soil contained in a given sample.

A study of the dependence of polarization and reflectivity on the degree of compaction, along with spectrophotometry of Apollo 12 soil and rocks, will be reported elsewhere (Briggs and O'Leary, in preparation).

ACKNOWLEDGEMENTS--We wish to thank Dr. Elizabeth Bilson for assistance with the sedimentation column work, Mr. Frank Briggs for assistance with optical studies, and Miss Joan Winters for assistance with electron microscope particle size counts. Mr. H. J. Eckelmann and Mr. S. M. Colbert helped in the design of the sedimentation column.

We wish to acknowledge gratefully the assistance given us by the Instrumental Analysis Research Department of the Corning

Glass Works with scanning electron microscope work.

Work on lunar samples was carried out under NASA Contract NASA NAS9-8018.

REFERENCES

Gold, T., Campbell, M. J. and O'Leary, B. T. (1970) Optical and High-frequency Electrical Properties of the Lunar Sample, Proc. Apollo 11 Lunar Sci. Conf., Geochim. Cosmochim. Acta Suppl. 1, Vol, 3, pp. 2149-2154. Pergamon.

LSPET (Lunar Sample Preliminary Examination Team) Preliminary examination of the lunar samples from Apollo 12. Science 167, 1325-1339.

Anders, E. Apollo 12 Lunar Science Conference (unpublished proceedings).

Campbell, M. J., and Ulrichs, J. (1969) Electrical Properties of Rocks and Their Significance for Lunar Radar Observations, J. Geophys. Res. 74, 5867-5881.

Evans, J. V. and Hagfors, T. (1968) Radar Astronomy, McGraw-Hill, New York.

Krotikov, V. D. and Troitsky, V. S. (1963) Radio Emission and the Nature of the Moon, Usp. Fiz. Nauk 81, 589-639.

O'Leary, B. and Briggs, F. (1970) Optical Properties of Apollo 11 Moon Samples, J. Geophys. Res. 75, 32, 6532-6538.

Hapke, B. (1968) Lunar Surface: Composition Inferred from Optical Properties, Science 159, 76-79.

Gehrels, T., Coffeen, T., and Owings, D. (1964) Wavelength Dependence of Polarization. III. The Lunar Surface, Astron. J. 69, 826-852.

Pellicori, S. F. (1969) Wavelength Dependence of Polarization. XIX. Comparison of the Lunar Surface with Laboratory Samples, Astron. J. 74, 1066-1072.

Briggs, F., and O'Leary, B., in preparation.

Fig. 1. The cumulative particle size distribution for the Apollo 11 and 12 bulk fines, determined from electron microscope data.

Fig. 2. The differential particle volume distribution for the Apollo 11 and 12 bulk fines, determined from electron microscope data.

Fig. 3. The differential particle size distribution for the Apollo 11 and 12 bulk fines, determined by the sedimentation column method.

Fig. 4. The differential particle size distribution for the Apollo 12 bulk and core samples, determined by the sedimentation column method.

Fig. 5. Differential particle volume distribution for the Apollo 11 bulk fines. Curve fits the electron microscope data, sedimentation data are also shown.

Fig. 6. Differential particle volume distribution for the Apollo 12 bulk fines. Curve fits the electron microscope data, sedimentation data are also shown.

Fig. 7. Dielectric constant measurements for two Apollo 12 powder samples and the Apollo 11 bulk sample, as a function of bulk powder density. Dielectric constant vs. density points for four solid lunar rocks are also shown.

Fig. 8. The variation with density of the absorption length in two Apollo 12 powder samples and the Apollo 11 bulk sample. Points for four solid rocks are also shown.

Fig. 9. (a) Reflectivity of the Apollo 11 and 12 soil vs. phase angle at .56μm wavelength for viewing angles $\varepsilon=0^\circ$ and 60°. (b) Color index B-V of the powder samples vs. phase angle for $\varepsilon=0^\circ$. Also plotted are (c) the reddening junction of the entire moon, as determined by Gehrels et al. (4), and (d) B-V values for a region of Mare Tranquillitatis.

Fig. 10. The polarization of the Apollo 11 and 12 powders vs. phase angle at .56μm wavelength for viewing angles $\varepsilon=0^\circ$ and 60°.

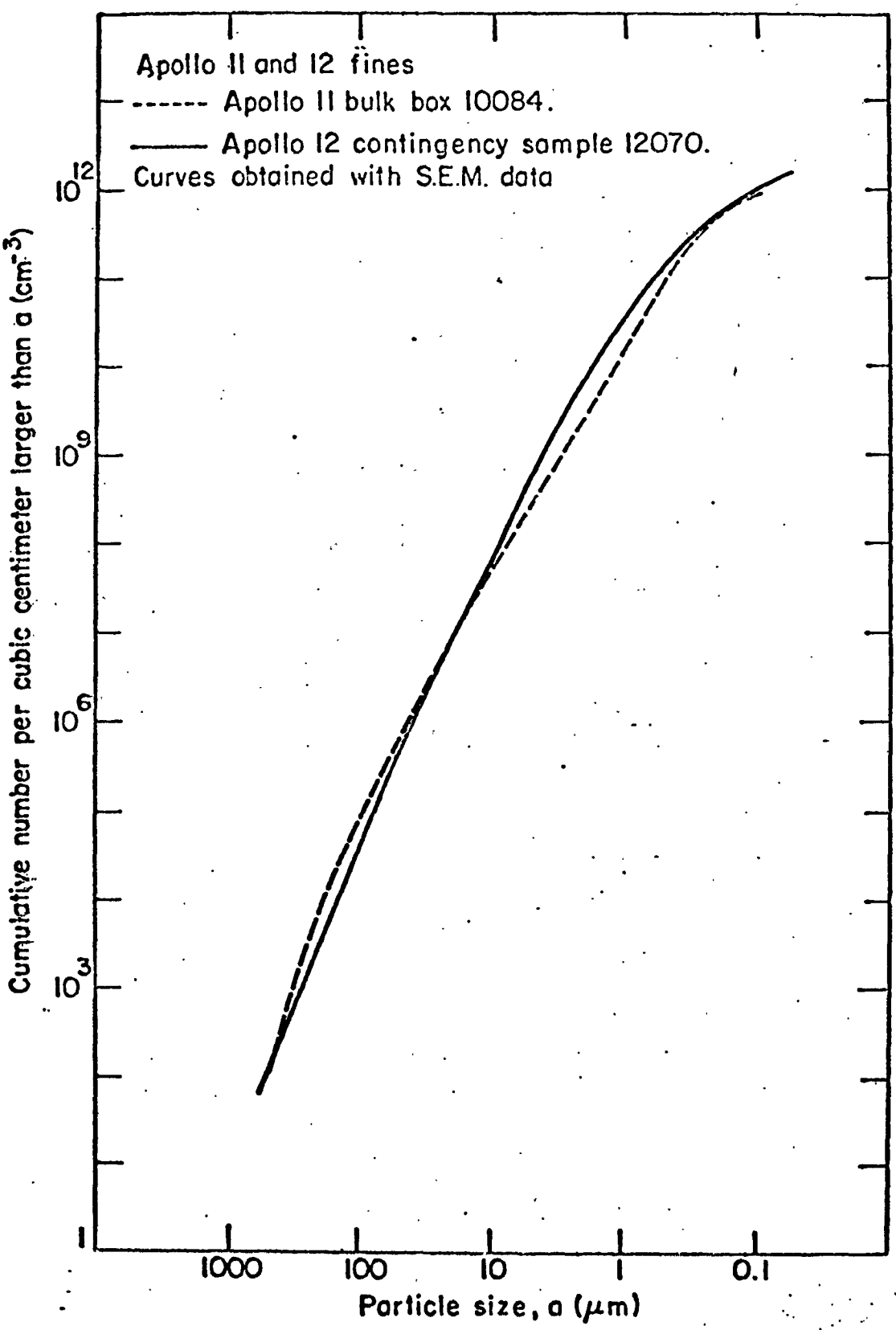
Apollo 11 and 12 fines
------ Apollo 11 bulk box 10084.
—— Apollo 12 contingency sample 12070.
Curves obtained with S.E.M. data
Cumulative number per cubic centimeter larger than a (cm⁻³)
10¹²
10⁹
10⁶
10³
1
1000
100
10
1
0.1
Particle size, a (μm)

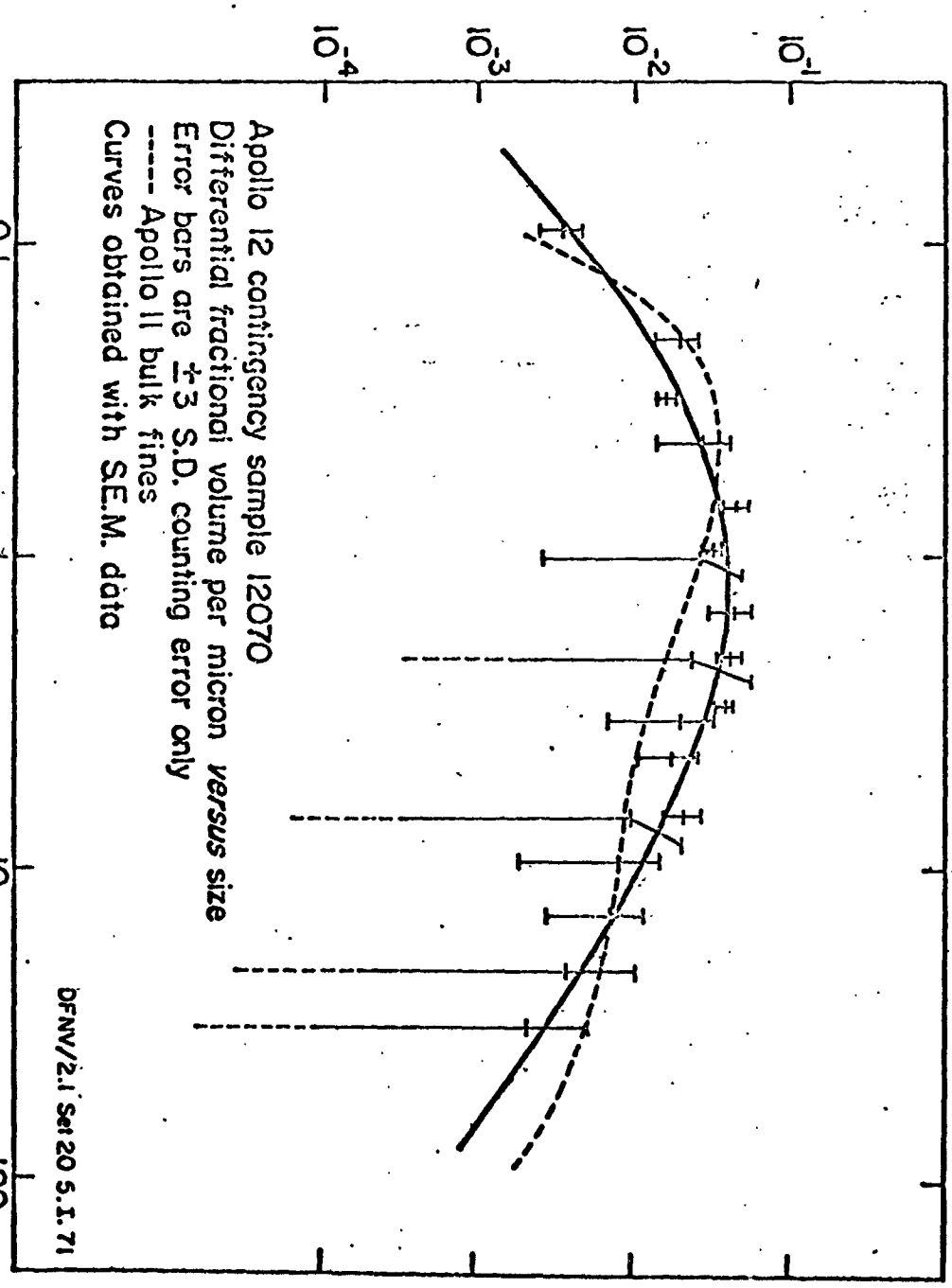
10^{-1}
10^{-2}
10^{-3}
10^{-4}
0.1
1
10
100
Particle size, μm
Apollo 12 contingency sample 12070
Differential fractional volume per micron versus size
Error bars are ±3 S.D. counting error only
----- Apollo 11 bulk fines
Curves obtained with S.E.M. data
DFNV/2.1 Set 20 5.1.71

Fig. 3

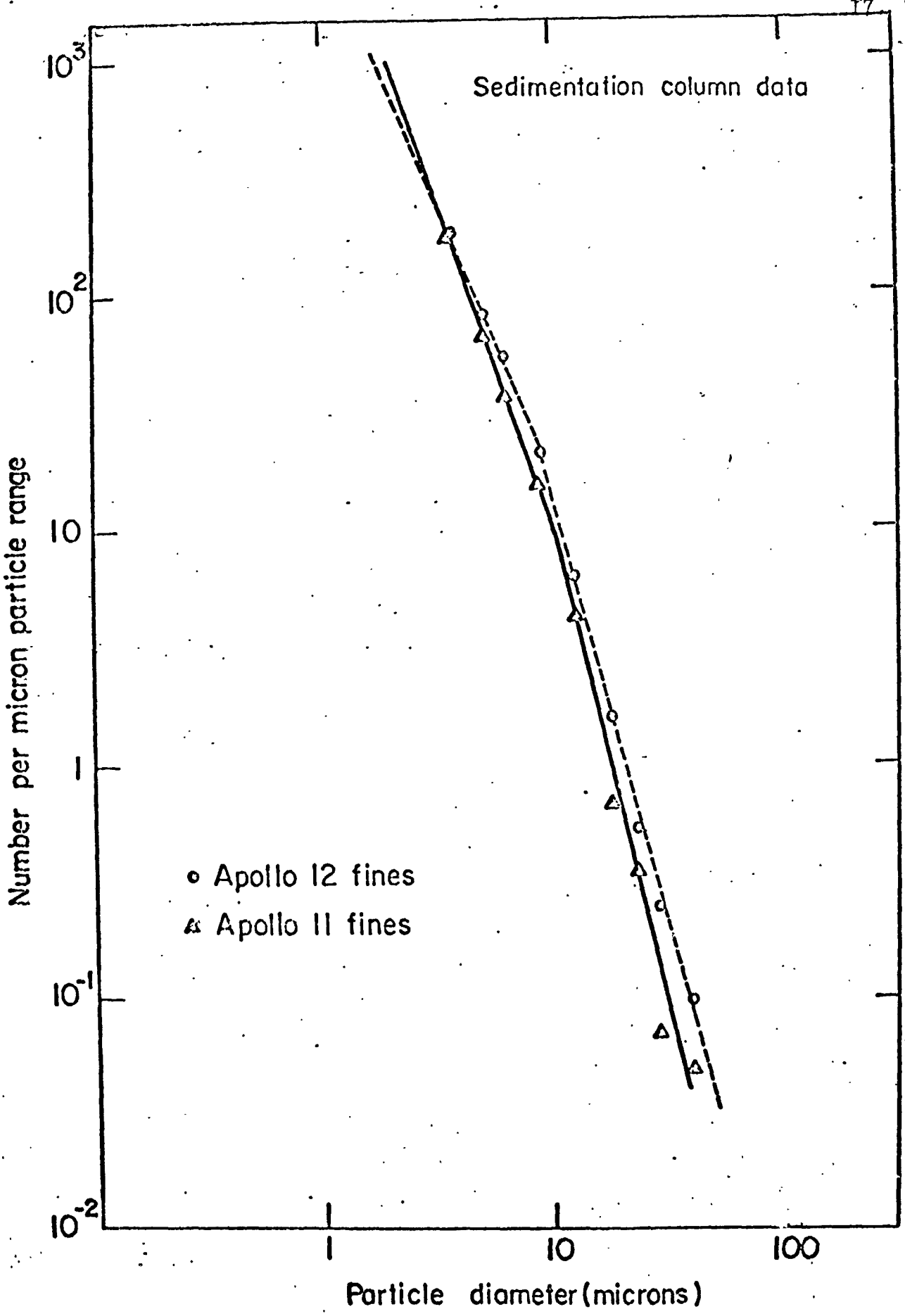
Sedimentation column data
Number per micron particle range
10^3
10^2
10
1
10^{-1}
10^{-2}
o Apollo 12 fines
Δ Apollo 11 fines
1
10
100
Particle diameter (microns)

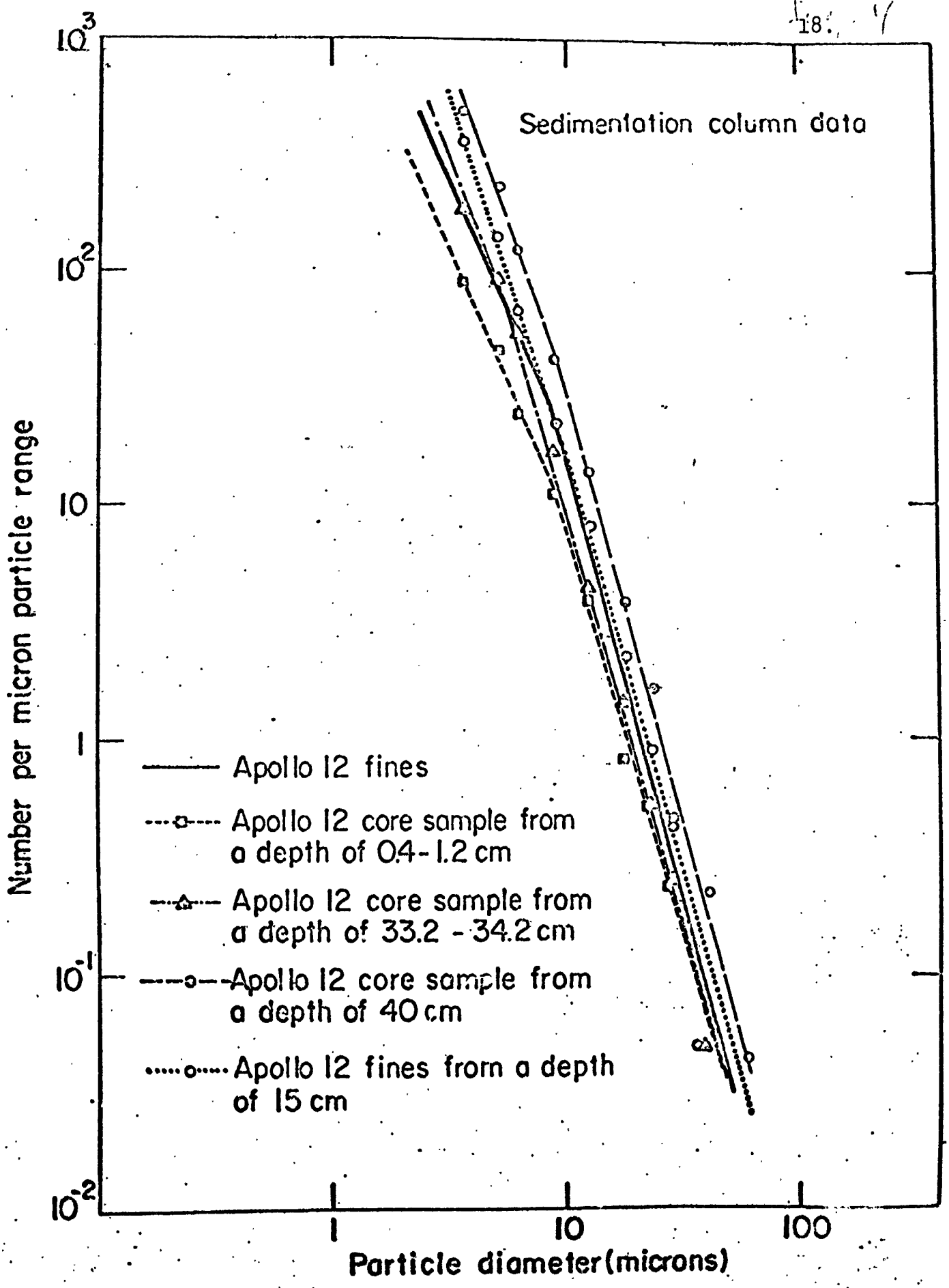
Sedimentation column data
Number per micron particle range
Particle diameter (microns)
10^3
10^2
10
1
10^{-1}
10^{-2}
1
10
100
Apollo 12 fines
Apollo 12 core sample from a depth of 0.4 - 1.2 cm
Apollo 12 core sample from a depth of 33.2 - 34.2 cm
Apollo 12 core sample from a depth of 40 cm
Apollo 12 fines from a depth of 15 cm

Fig. 5

19.

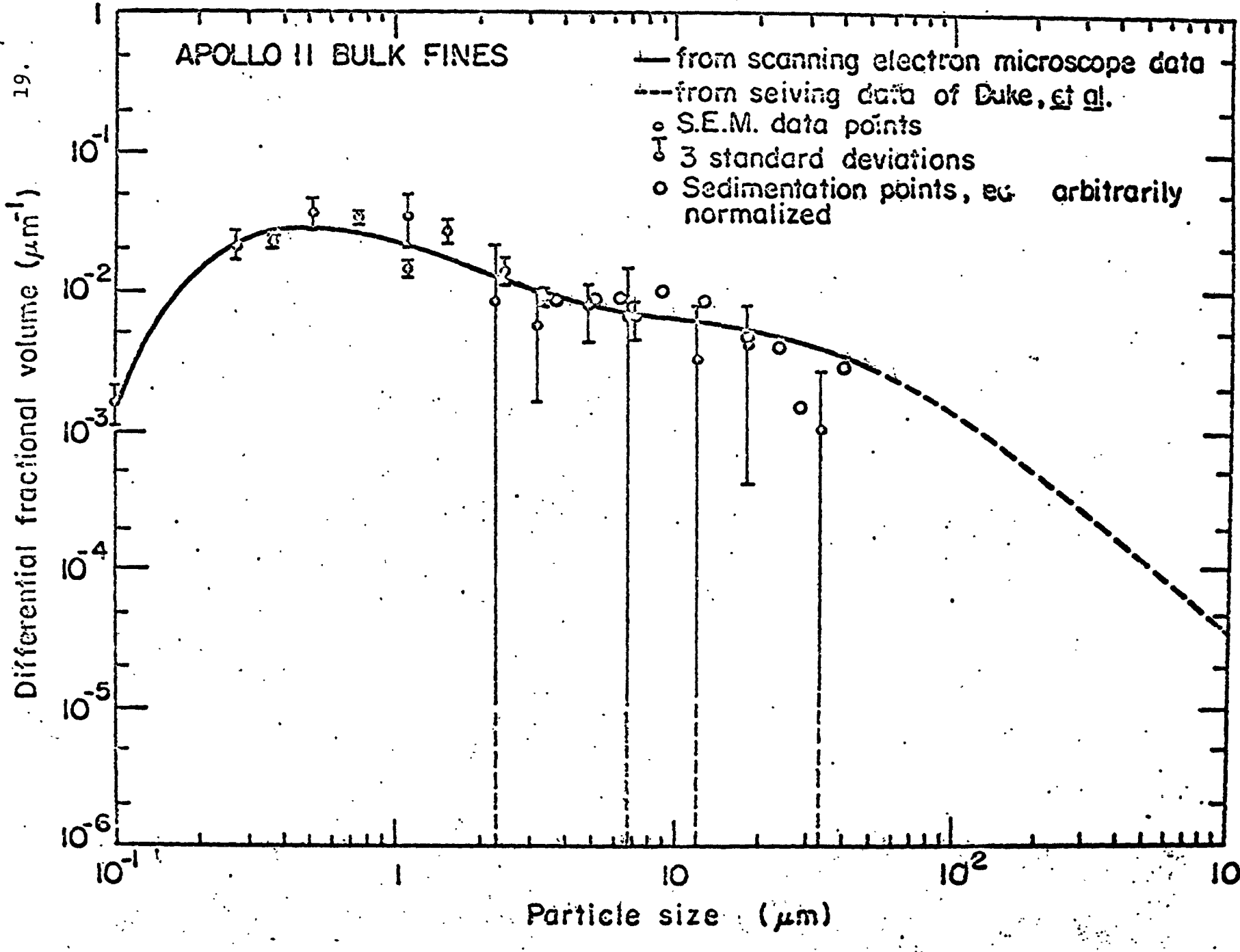
APOLLO 11 BULK FINES
—from scanning electron microscope data
---from seiving data of Duke, et al.
S.E.M. data points
3 standard deviations
Sedimentation points, eq. arbitrarily normalized
Differential fractional volume (μm^{-1})
Particle size (μm)
1
10^{-1}
10^{-2}
10^{-3}
10^{-4}
10^{-5}
10^{-6}
10^{-1}
1
10
10^{2}
10^{3}

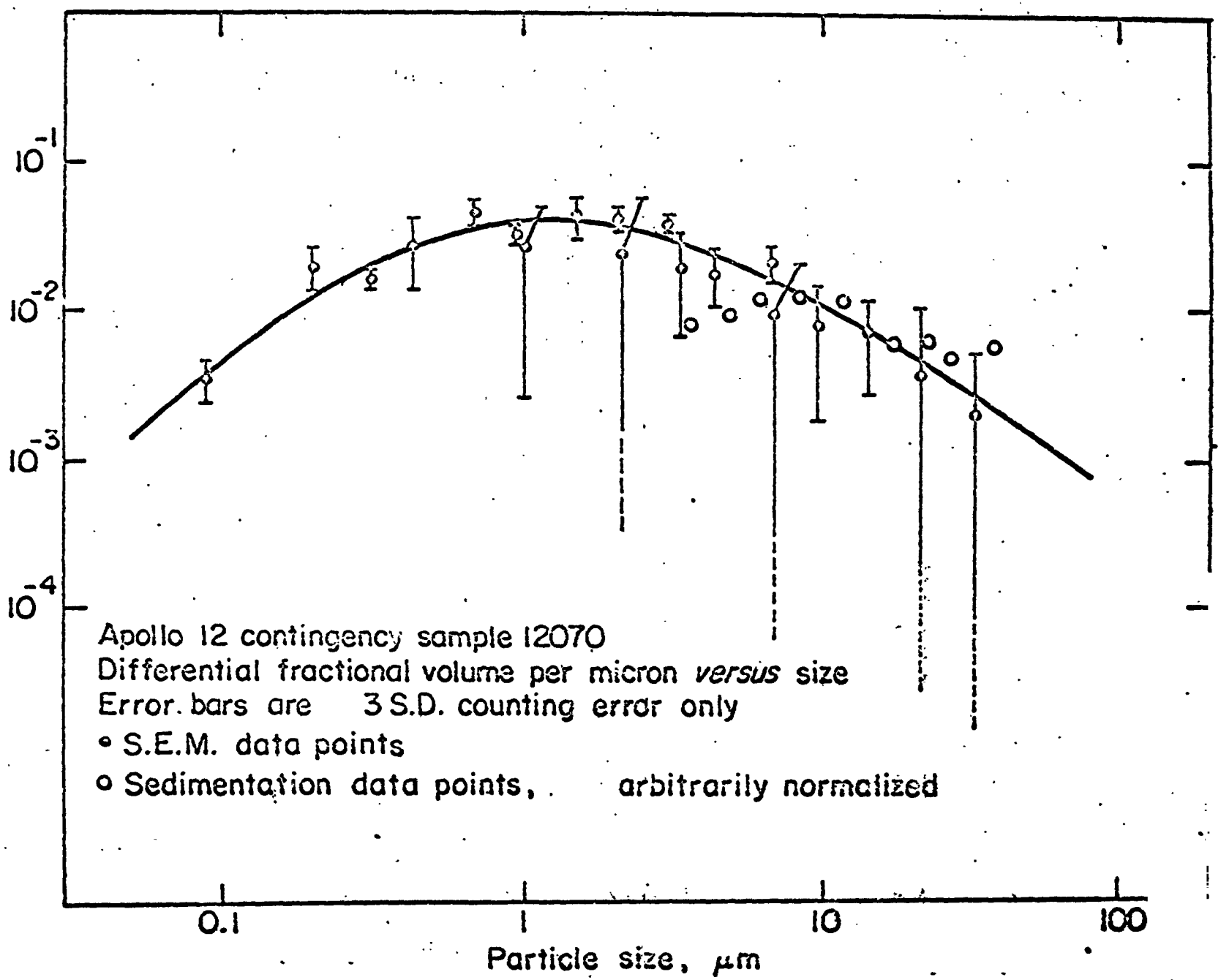
10^{-1}
10^{-2}
10^{-3}
10^{-4}
0.1
1
10
100
Particle size, μm
Apollo 12 contingency sample 12070
Differential fractional volume per micron *versus* size
Error bars are 3 S.D. counting error only
• S.E.M. data points
o Sedimentation data points, arbitrarily normalized

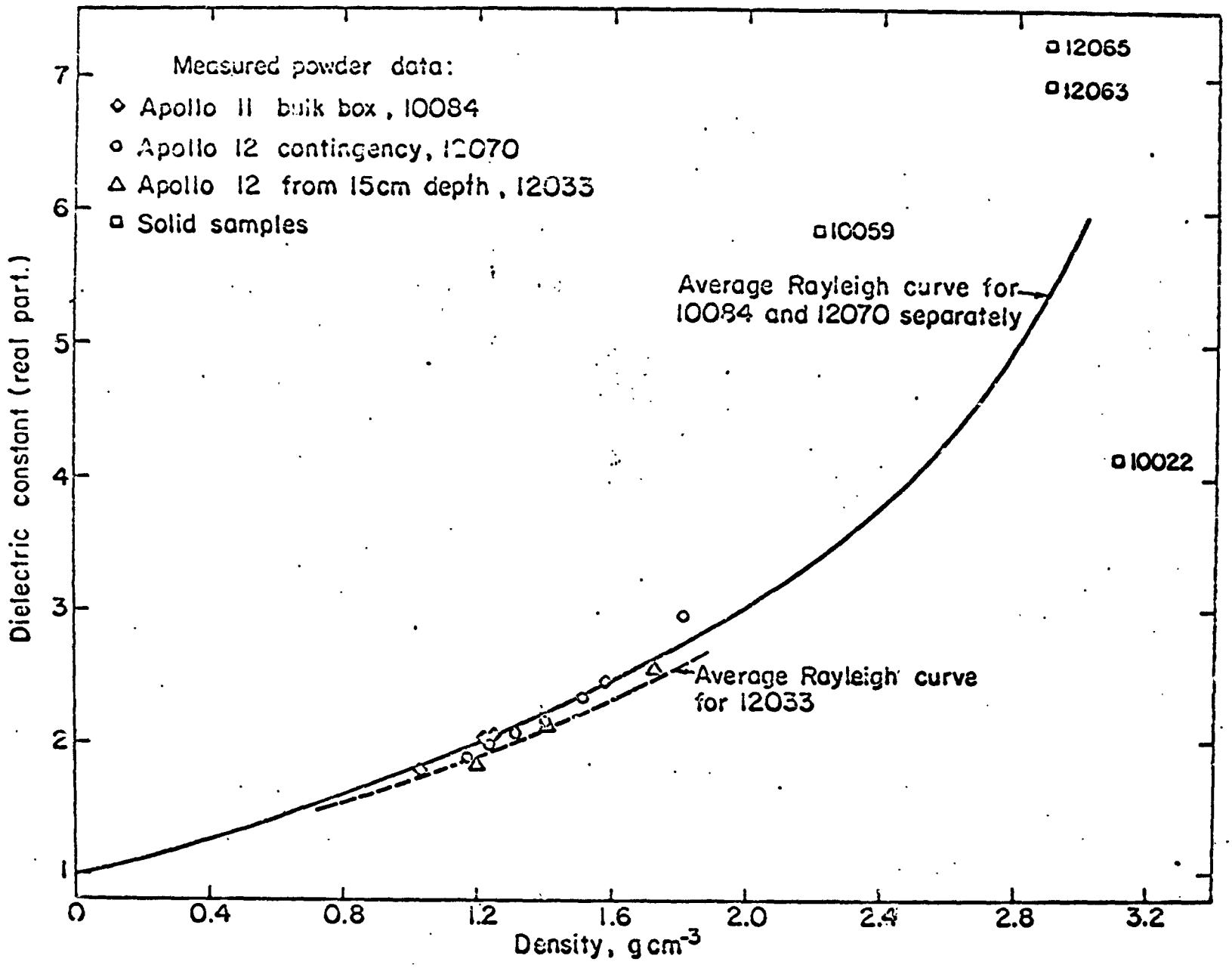
Measured powder data:
◇ Apollo 11 bulk box, 10084
○ Apollo 12 contingency, 12070
△ Apollo 12 from 15cm depth, 12033
□ Solid samples
□12065
□12063
□10059
Average Rayleigh curve for 10084 and 12070 separately
□10022
Average Rayleigh curve for 12033
Dielectric constant (real part.)
Density, g cm⁻³
1
2
3
4
5
6
7
0
0.4
0.8
1.2
1.6
2.0
2.4
2.8
3.2

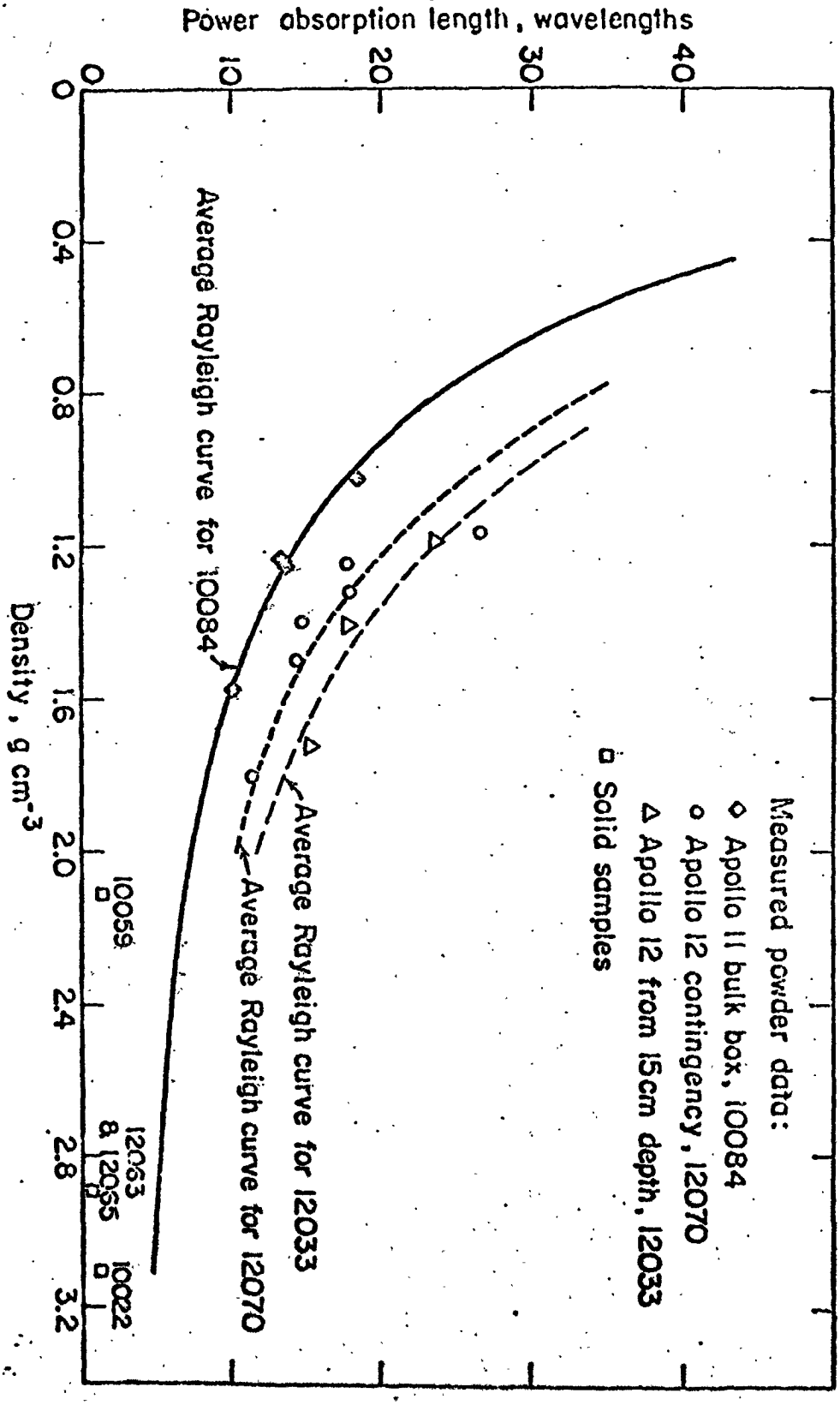
Power absorption length, wavelengths
0
10
20
30
40
0
0.4
0.8
1.2
1.6
2.0
2.4
2.8
3.2
Density, g cm⁻³
Average Rayleigh curve for 10084
Average Rayleigh curve for 12033
Average Rayleigh curve for 12070
10059
12063
& 12065
10022
Measured powder data:
◇ Apollo 11 bulk box, 10084
o Apollo 12 contingency, 12070
△ Apollo 12 from 15cm depth, 12033
□ Solid samples

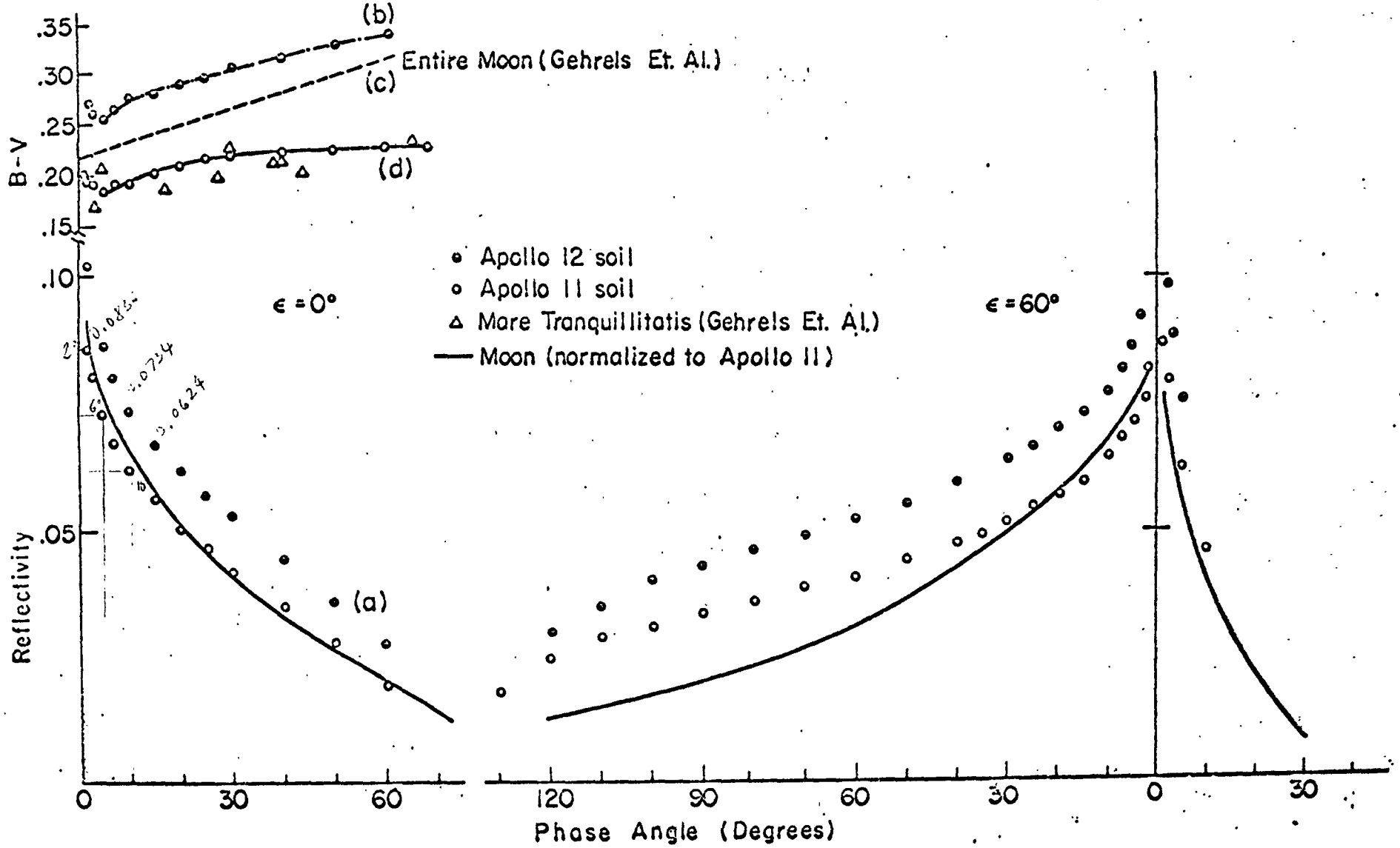
(b)
Entire Moon (Gehrels Et. Al.)
(c)
(d)
B-V
.35
.30
.25
.20
.15
.10
.05
Apollo 12 soil
Apollo 11 soil
Mare Tranquillitatis (Gehrels Et. Al.)
Moon (normalized to Apollo 11)
ε = 0°
ε = 60°
0.085
0.0724
0.0624
(a)
Reflectivity
0
30
60
120
90
60
30
0
30
Phase Angle (Degrees)

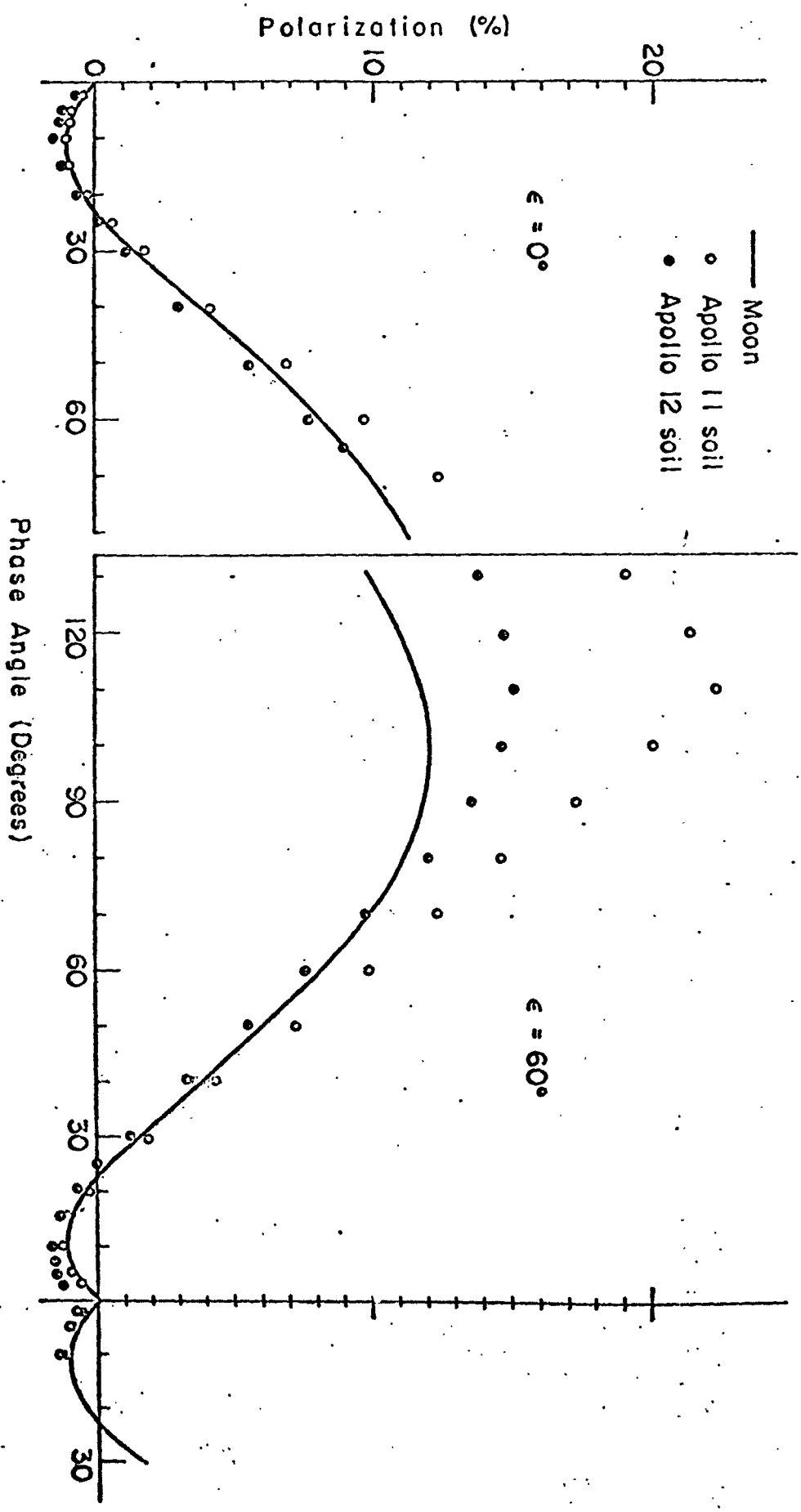
Polarization (%)
0
10
20
30
60
Phase Angle (Degrees)
120
90
60
30
0
30
ε = 0°
ε = 60°
Moon
Apollo 11 soil
Apollo 12 soil

N72-24871

Gold, Campbell, O'Leary -

OPTICAL AND HIGH FREQUENCY ELECTRICAL PROPERTIES OF THE LUNAR SAMPLE

Reflectivity and polarization laws for the powder sample and its spectrum are close to the mean for the lunar maria. Solid samples show a marked absorption feature at 1 micron. The low albedo appears to be due to a surface coating on dust grains rather than volume absorption. The high frequency electrical properties resemble those of a fine powder made from typical dense terrestrial rocks, and are consistent with previous ground-based radar estimates. The differential mass spectrum is almost constant from 100μm particles down to 0.1μm; most particles are smaller than 0.3μm. Their shapes disclose a variety of generation processes.

The analysis of lunar dust and rock chip samples carried out in the lunar laboratory of the Cornell Center for Radiophysics and Space Research has been concerned with the optical and electrical properties of the sample and their relation to those known for the lunar surface as a whole, and with the questions surrounding the origin of the lunar dust. The salient points that have emerged are the following:

1. The optical scattering law and polarization properties of a surface of lunar dust generally correspond closely to these properties as observed for the moon as a whole. The rock chip sample shows a strong absorption feature at 1 micron which is not prominent in the lunar scattered light. It is probable therefore that most of the lunar surface is covered with a material similar to the powder that was investigated.

2. The dielectric constant is within the range that had been estimated for the moon as a whole by radar methods.

3. The particle size distribution indicates that the differential mass spectrum as a function of radius is constant from 100 microns down to 1000 Ångstroms. The shapes of the particles indicate a variety of sources; some have the sharp edged shapes characteristic of fracture, others are rounded, indicating processes of melting or condensation. Some cannot readily be attributed to either of these mechanisms.

4. The darkness of the lunar dust is mainly due to dark surface deposits on the grains, probably metallic, rather than absorptivity of the bulk material.

The Optical Measurements

The optical scattering law as a function of phase angle and the optical polarization law were measured with the same instrument and in the same manner in which many sample powders had been measured in the past (1). The lunar powder proved to resemble, both in appearance and in the measured optical properties, the lunar maria as observed from the earth and the terrestrial powders previously advanced (1) as being most closely representative of the moon. These powders also proved to be similar under optical microscope examination. The particle size was similar, the great majority of the particles being less than 10 microns. The adhesion of the small particles to each other indeed created the "dendritic growth" appearance under the microscope that has been given the name "fairy castles". It appears that the large part of the pronounced lunar opposition effect, i.e. the brightness surge toward zero phase, can be attributed to the shadow casting of this lacy surface structure.

Figures 1 and 2 summarize the optical properties of the Apollo 11 samples. Each data point represents the mean of several observations of different portions of a sample, and the measurements repeated very well. In Figure 1 the photometric phase function of the lunar dust sample is generally steeper than the mean lunar case (1) for phase angles less than 15°, but the difference is very small. The polarization

versus phase angle curve (Fig. 1) also demonstrates the similarity of the dust sample to the moon as a whole, but, again, there are minor differences; the crossover from negative to positive polarization occurs at a lower phase angle, and polarization in the positive branch is greater.

The normal albedo of the dust sample at 5600 Å was measured as 10.2% ± 0.2%. This value is in close accord with the value 9.96% for the Apollo 11 site as derived from Apollo 10 orbital photography (2). Moreover, in the hemispherical reflectance measurements performed on a Cary 14 spectrophotometer, the albedo values of the dust sample in the visible and near infrared were similar to lunar maria values obtained from earth-based observations. Both spectra are featureless with a steady climb in albedo from ~ 0.3 to 1.5μm (Figure 2). Lunar rock chip samples were also measured on the spectrophotometer and a strong absorption band, not present in the powder sample, appeared near 1 micron. A weak band in this region has previously been suggested from earth-based observations of the moon (3). Further details of the optical properties of the Apollo 11 samples will be presented in the near future (4).

Darkness of the Lunar Dust

Rock powders in the size range of a few microns tend to be very light in color. The opacity of most rocks is too low to absorb much of a light ray, which is generally scattered out of the surface after having traversed only a few microns of material. It has been a long-standing problem to account

for the very low albedo of the lunar surface in view of the indication of a very small particle size coming from the optical scattering and polarization properties, since even the darkest rocks tend to be quite light when powdered. We had previously, in this laboratory, undertaken sputtering experiments with kilovolt protons and alpha-particles on powdered rock surfaces, which have indicated darkening. It has been suggested that this darkening was due to the deposition of reduced metals, perhaps chiefly iron, on the surface as a result of the dissociation by the sputtering process, the partial escape of the oxygen, and the slowness of surface recombination limited by diffusion.

Metallic surface coatings of as little as 30 Ångstroms can provide much opacity but would make an insignificant contribution only to the bulk chemical composition. We have seen strong evidence for such coatings, but we have not yet been able to do an adequate chemical analysis of them. Whether they are indeed the result of sputtering, or of other metal evaporation (vacuum plating) processes, or whether perhaps just the reduction by the hydrogen of the solar wind produced metallic surface layers, is not yet clear. However, we have had the following indications of the presence of metallic layers.

We observed under the microscope that some larger particles in the size range 50 to 200 microns that could be found in the lunar soil sample had a metallic appearance, sometimes over only a certain part of their surface. Some particles could be clearly seen as translucent glass with a well-defined area

appearing metallic. One sphere, for example, looked a honey-colored glass from one side, but looked like a steel ball from the other. When treated with the common acids that attack metals, hydrochloric and nitric, the appearance of the metallized coating was generally reduced but not completely removed. Hydrofluoric acid generally tended to remove the entire metallic appearance, even before a visible erosion of the particle had taken place.

For the majority of the material an optical examination is not feasible because the particles are too small. Nevertheless, when the same acids were applied to a microscopic sample of fine powder it quickly turned to a very much lighter, almost white, appearance. It seems likely therefore that in the finer material a metallic surface coating is also normally present and responsible for the low albedo.

Particle Size Distribution

The measurement of a particle size distribution for such small grains is not an easy matter. The cohesion of the grains prevents the analysis of the smaller sizes by sieving as is pointed out by the preliminary investigators (5). We have employed three techniques. One is that of making microscope slides of the powder mixed into a transparent varnish and smeared out into a thin layer, permitting the counting of particles with an oil emersion microscope down to about 2 microns. Secondly, a water sedimentation column has been

constructed in which the descent of particles as small as 1 micron can be photographically registered. In addition the size distribution of the smallest particles has been determined from the scanning electron micrographs referred to below. The three methods give consistent results which are presented in Fig. 3.

Scanning Electron Microscope Observations

The detailed shapes of particles can be seen to a resolution of 300 Angstroms in numerous scanning electron microscope pictures that were taken to see whether the origin of the material was revealed by the particle shapes.

Our studies indicate that a variety of different effects have been active in producing the fine material. Some particles show spherical and rounded shapes suggesting condensation from a vapor or freezing of a liquid in free fall. Others are undoubtedly the result of fracture, and display the characteristic sharp edged angular appearance. They lack in general any obvious indication of a crystalline structure, as neither cleavage planes nor preferred angles are seen. It would appear that most of the fractured material is amorphous, or, if any of it is crystalline, that the size of the crystals is below the resolution limit.

The spherical or compact round shapes seem are less frequent but may form a continuous sequence from the hundred micron range down to very small sizes. The great majority

of particles in the ten to one micron size range have, however, more intricate shapes that are not readily understood. There are many rounded surfaces, and yet the shape as a whole is not compact. Elongated objects with rounded ends, surfaces where the sense of the curvature changes over many times, rough spots occurring in smooth surfaces, and various other features argue against any single explanation, e.g., liquid droplets, condensation or fracturing. Additional processes such as erosion by sputtering, partial melting and partial evaporation need to be considered, and scanning electron microscope study of these mechanisms is needed before all the responsible processes can be identified.

Electrical Measurements

Measurements were carried out using the identical technique employed for determining the electrical properties of terrestrial rock powders (6). The dielectric constant and loss tangent of lunar dust at several stages of compaction were measured at 450 MHz. The measurement in each case included a measurement of the density of the sample, and the porosity was calculated from the quoted specific gravity of the rock of which the powder is composed (5). The dielectric constant and absorption length are shown in Fig. 4, and are consistent with the values deduced from ground-based radar and radiometric observations respectively. As with terrestrial rock powders, the permittivity and loss tangent as a function of porosity follow the Rayleigh Mixing

Formula and, by extrapolation, suggest a permittivity for the solid rock of the same composition as the lunar dust which is near the average of dense terrestrial rocks (about 7). The permittivity is about 3 for the dust at a typical "loose packing" porosity of 0.4. The absorption length at the same porosity, in this sample, is about 10 wavelengths.

We are very grateful to the Corning Glass Works for the assistance given us in the preparation of the electron micrographs. This work was supported by NASA Contract NAS 9 8018

T. Gold
M. J. Campbell
B. T. O'Leary

Center for Radiophysics and Space Research, Cornell University, Ithaca, New York.

REFERENCES AND NOTES

1. B. Hapke, Science 159, 76 (1968).

2. R.L. Wildey and H.A. Pohn, Astrophys. J. 158, L129 (1969).

3. R.B. Wattson and R.E. Danielson, Astrophys. J. 142, 16 (1965); R.G. Tull, Icarus 5, 505 (1966).

4. B.O'Leary and F. Briggs, submitted to Science.

5. D.H. Anderson et al., Science 165, 1211 (1969).

6. M.J. Campbell and J. Ulrichs, J. Geophys. Res. 74, 5867 (1969).

7. This work was done under NASA contract NAS9-8018. We thank Paul Shapshak, F. Briggs and J. Winters.

FIGURE CAPTIONS

Fig. 1. The dependence of reflectivity and polarization on phase angle at 5600 Å wavelength and at normal viewing. The Moon curves are taken from Wattson & Danielson

Fig. 2. The spectral reflectance of Apollo 11 lunar samples. The Moon curve is taken from Hapke (1) with arbitrary normalization of reflectivities.

Fig. 3. The differential particle size distribution for the bulk sample.

Fig. 4. The dielectric constant and absorption length of the bulk sample at 450 MHz as a function of the powder density. The solid curves are the Rayleigh formula (6).

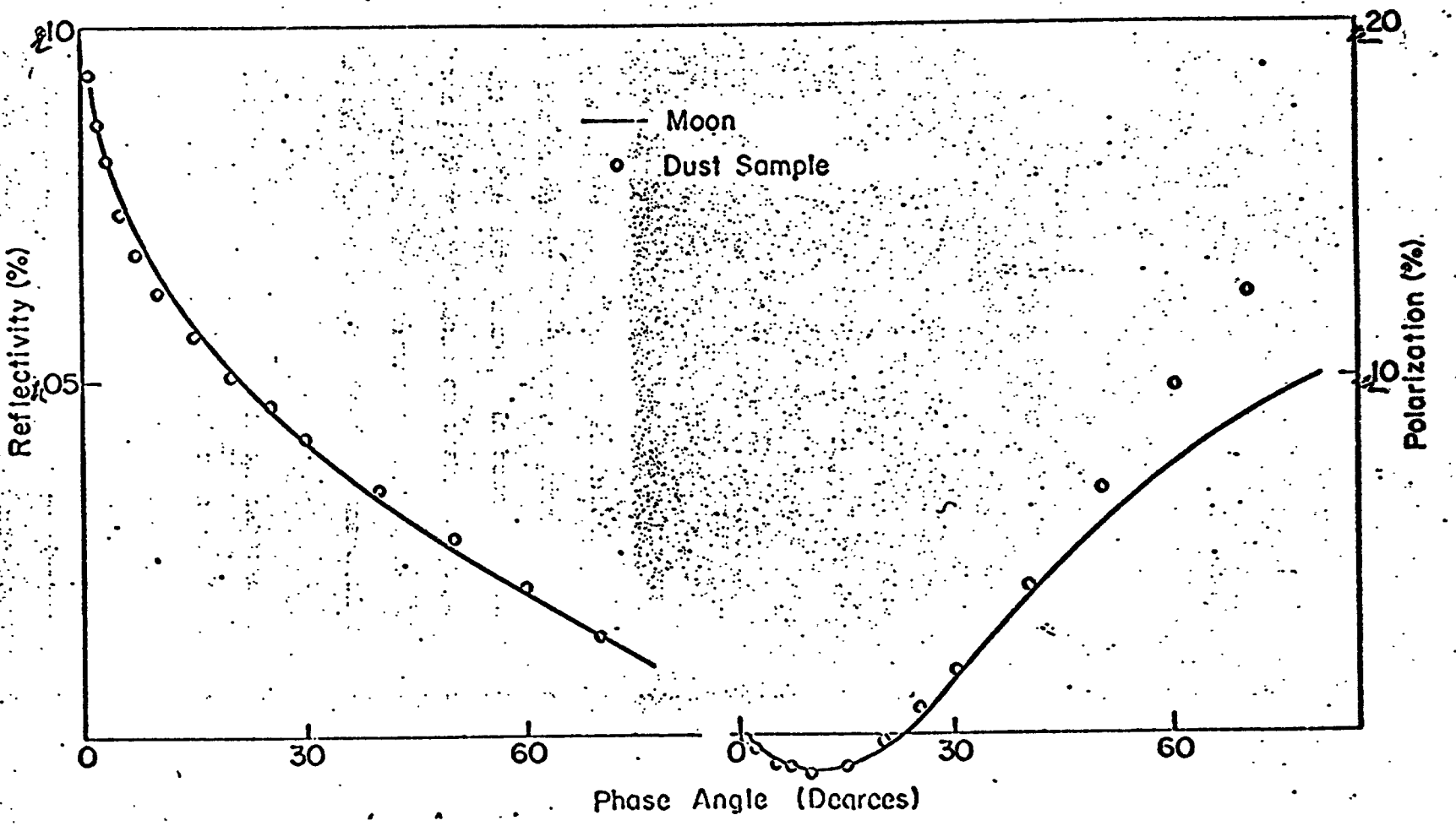

Fig. 1. The dependence of reflectivity and polarization on phase angle at wavelength of 5600 Å and at normal viewing. (Curve for the moon from Hapke (1968), with arbitrary normalization of reflectivities.)

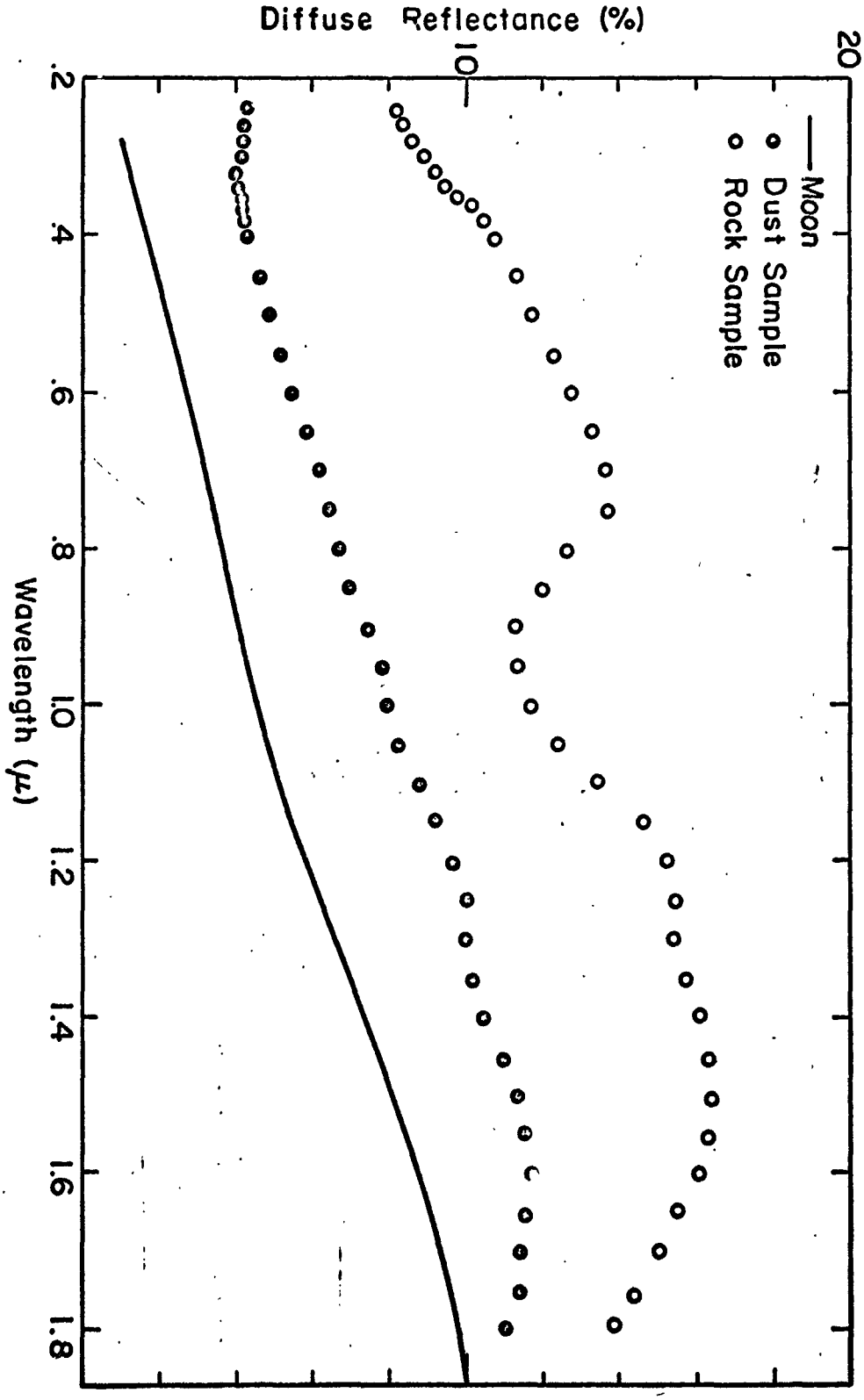
Diffuse Reflectance (%)
10
20
.2
.4
.6
.8
1.0
1.2
1.4
1.6
1.8
Wavelength (μ)
Moon
Dust Sample
Rock Sample

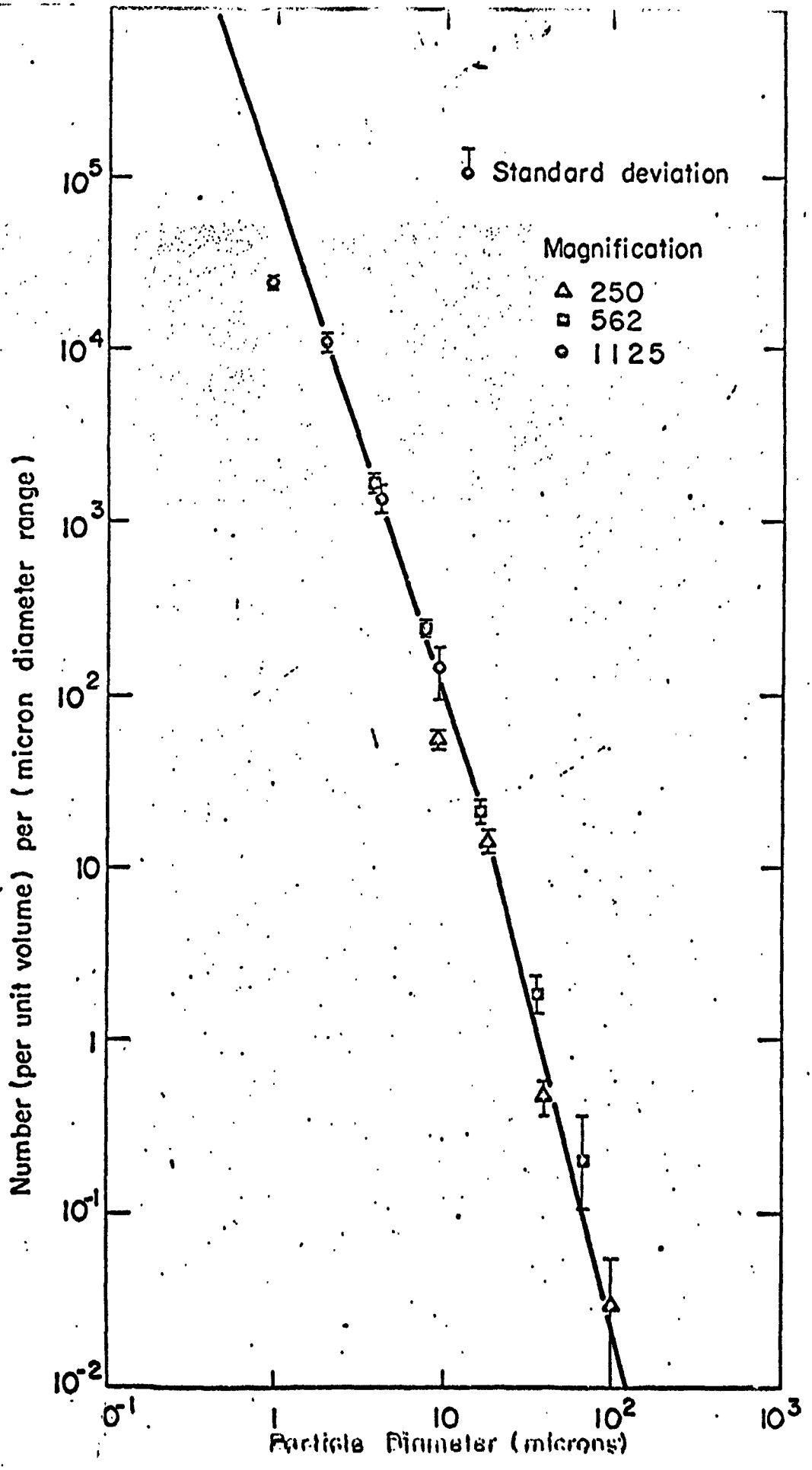
Standard deviation
Magnification
250
562
1125
Number (per unit volume) per (micron diameter range)
Particle Diameter (microns)
10^5
10^4
10^3
10^2
10
1
10^{-1}
10^{-2}
10^{-1}
1
10
10^2
10^3

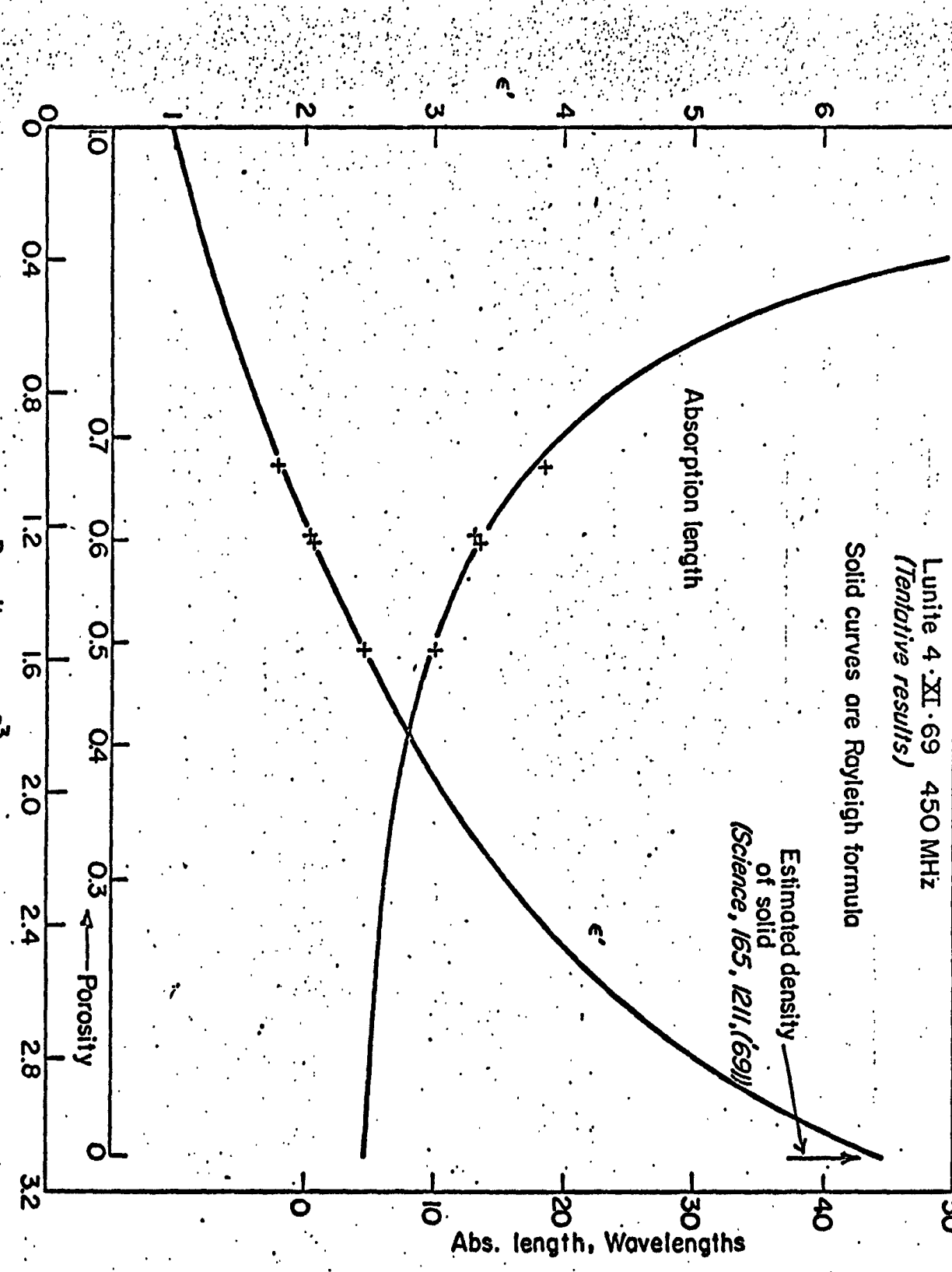
Lunite 4·XI·69 450 MHz
(Tentative results)
Solid curves are Rayleigh formula
Estimated density of solid (Science, 165, 1211, (69))
Absorption length
ε'
ε'
Abs. length, Wavelengths
Density, ρ cm⁻³
Porosity
0
0.4
0.8
1.2
1.6
2.0
2.4
2.8
3.2
0.7
0.6
0.5
0.4
0.3
1.0
1
2
3
4
5
6
10
20
30
40
50